

Characterization of Spatial Reflection Co-efficient for Ground-to-Aircraft and Satellite-to-Aircraft Communication

Muhammad-Yasir Masood Mirza¹, Noor M. Khan¹, Abid Jamal¹, and Rodica Ramer²

¹ Department of Electrical Engineering
Capital University of Science and Technology, Islamabad, 44000, Pakistan
yasir@arwic.com, abidjamal010@gmail.com, noor@ieee.org

² School of Electrical Engineering and Telecommunications
University of New South Wales (UNSW), Sydney, Australia
ror@unsw.edu.au

Abstract — Because of high sensitivity and long range capability in modern radars, Radar Cross-Section (RCS) is considered to be one of the most important factors in the performance evaluation of stealth technology and for defense applications, especially those that deal with airborne weapon system. In this paper, a concrete relationship is established between RCS and spatial reflection coefficient (SRC) for the two proposed scenarios, i.e., Satellite-to-Aircraft and Ground-to-Aircraft. Geometrical models of the two proposed scenarios are presented for the evaluation of correct incident angles of impinging waves on the surface of aircraft and their corresponding RCS observations. For numerical computation of RCS, a simulation tool POFACET® [1] based upon the methodology of Physical Optics (PO) and a FACET-based aircraft A380 model is used for the designed scenarios. In both the scenarios, the result shows that the aircraft has strong signal reflecting properties which results in the form of RCS to radar receiver or neighboring aircrafts. Further, the RCS results are used to evaluate the spatial reflection coefficients of scattered signal received at any neighboring signal receiving unit. Comparison between RCS and SRC validates that these terms have similar scattering behavior and can be used interchangeably for performance evaluation of communication system models. From the result, it is evident to mention that flying aircrafts are one prominent source of interference which may provide interference to its neighboring aircrafts and as a result degrades their communication performance.

Index Terms — Bistatic radar cross-section, ground-to-aircraft, physical optics, radar cross-section, satellite-to-aircraft.

I. INTRODUCTION

RADAR (Radio Detecting And Ranging) is a device that reveals the presence of a target within its range of coverage. The post-processing capability of a RADAR on the received reflected Electromagnetic (EM) waves (echos or radar returns) extracts the information of the target's direction, range, velocity, orientation and other classifying characteristics. When the radar's transmitted EM waves impinge on target's surface, the reflecting surface of the object radiates EM energy in all directions. The radiated energy depends upon the target size, physical shape, orientation and reflecting properties of the surface. These all can be put together to specify target's identification parameter known as Radar Cross Section (RCS). Quantitatively, it can be termed as a fictitious surface area which explains the intensity of EM wave reflected back to the radar's receiver antenna. The RCS is a measure of an object's reflecting ability which exploits the visibility of the intended target towards the RADAR. Due to high sensitivity and long range capability in modern RADARs, RCS is considered as one of the most important factors in the performance evaluation of stealth technology and for airborne weapon systems [2,3]. In the designing of modern fighter aircraft, the performance of stealth technology and the visibility of an aircraft highly depend on the results and measurements of RCS. In order to accurately predict the RCS of a target, it is necessary to analyze the factors that affect its behavior, such as material, incident angle, radar signals wavelength, size of the target, radar operating frequency and target's orientation.

The correct evaluation of the RCS and its prediction is imperative in designing of high-performance radars as well as for aircrafts having low visibility (stealth) towards the radar. Such problems deal with the

techniques available in electromagnetic computational theory. It is well established from the literature that the behavior of electric and magnetic fields is governed by Maxwell's equations. In the literature, two main computational electromagnetic methods have been developed to deal with the electromagnetic problems: time-domain methods and frequency-domain methods. As both of the domains interrelate with each other by the Fourier transform which makes them different in solution procedure, therefore, both possess different strengths and applicabilities. In the problems, when it is required to observe the electromagnetic scattering from objects larger than the wavelength, the weak convergence properties of solutions based on Rayleigh's method make it desirable to use high-frequency asymptotic methods [4]. Moreover, the approximation procedure of high-frequency asymptotic (HFA) techniques make it prevalent to be used for a large group of problems as compared to those which can be handled with low-frequency methods. Applying computational electromagnetic method in frequency-domain requires a solution of system of linear equations for each frequency and once the solution matrix is inverted or factorized, it can be used repeatedly to obtain the solutions of all excitations. This makes frequency-domain methods attractive for problems in which it is required to consider many excitations [4]. HFA techniques [5,6] such as Physical Optics (PO), Geometric Optics (GO), Physical Theory of Diffraction (PTD) and the Geometrical Theory of Diffraction (GTD) require correct modeling of the object geometry. These approaches incorporate scattering mechanisms to estimate the reflectivity of the target in both qualitative and quantitative manner. Since, it is not possible to acquire the exact dimensions of the intended object always, therefore, in such cases the requirement of geometry limits the applicability of HFA techniques. On the other hand, numerical approaches include Method of Moments (MoM) [7], the Fast Multipole Method (FMM) [8], the Finite Difference Time-Domain (FDTD) [9,10] Method and Transmission-line Matrix (TLM) [11]. In comparison to HFA techniques, numerical approaches are geometry-independent and of a general nature which can be applied to any object within the limitations of computer processing capability.

In [12], the authors fitted the Chi-square distribution on aircraft's RCS measurements by evaluating its statistical parameters. From the results, it was concluded that the statistical parameters have a strong dependency on radar operating frequency, the geometry of the aircraft and on aspect angles. On the basis of these statistics, aircraft detection probabilities were also estimated and concluded with the fact that the average value of RCS highly effects the detection probability than the normalized value of RCS. In [13], the authors measured RCS of commercial aircrafts along different flight routes to observe the impact of RCS fluctuations

with respect to aspect angles and their dependency on the classification of aircrafts. From the results, it was concluded that the change in aspect angle substantially influence RCS measurements and as a result provides fluctuations in RCS. In situations, when the wavelength of radar's signal is smaller than object's dimension, it will provide higher rate of fluctuations in RCS. Hence, for correct modeling and simulations, spatial RCS variations must be incorporated. In [14], the authors presented an implementation procedure of measuring RCS of aircraft and pointed some essential tradeoffs between its accuracy and computational cost in modeling and simulation of RCS related applications. Seven interpolation schemes were considered for the generation of continuous RCS samples, among them spline interpolation method was proved best for originating new data points with less interpolation error. To accelerate the computation efficiency of monostatic RCS, a number of fast and efficient interpolation techniques have been reported in the literature [15-19] to reduce the time and memory requirement of RCS calculations.

It is evident from the literature that a signal received at the receiver not only contains a direct Line-of-Sight (LoS) signal component but also contains multiple reflected copies of the transmitted signal that arrive at the receiver with different delays [20]. The delayed reflected copies are basically the result of reflections, refraction, diffraction or scattering from terrains, trees, mountain or in fact anything present between the transmitter and receiver ends. The reflectance properties of every object vary depending upon its permittivity and permeability levels. Furthermore, the relation between reflected and incident field is usually described by Fresnel equations, which depends upon the permittivity, conductivity of the surface and frequency, incident angle and polarization of the incident waves. Hence, the reflection coefficient better describes the amount of radiated energy in one term by accumulating all the reflecting properties of the surface and the wave. Being the same signal reflecting phenomenon, the signal transmitted through satellites/ground stations towards an aircraft of interest may get reflected through its proximate aircrafts. As a result, the aircrafts flying in the proximity of aircraft of interest will act as scatterers and will provide interfering signals which may degrade the communication performance. This concept can be legitimized by analyzing the work performed in [21]. Prior to this work, it was generally assumed that the signal reflection from the taxing aircrafts at airports provides interference to the Instrument Landing System (ILS) localizer which degrades its localization efficiency; however, no measurement campaign was conducted to validate/invalidate this thought. In [21], the authors presented a scaled measurement setup to evaluate the quantitative measure of interference to an ILS-localizer due to reflections from large-size aircrafts like Airbus® A380 and Boeing® B747 aircrafts. The

bistatic RCS results show that both the aircrafts provide interference to ILS-localizer, however, A380 tends to have a slightly larger disturbing influence to ILS-localizer as compared to B747. Thus reflections of signals from the aircraft's body can be interpreted as a main source of interference in satellite-to-aircraft communication and ground-to-aircraft communication, in which the flying aircrafts act as scatters. Since, the RCS and the reflected signals from the aircraft's body gives the same concept, therefore, a relationship can easily be made between these two terms. Both the terms depend on the incidence angle, material properties, signaling frequency, polarization and observation angle. In literature, a lot of work has been proposed to acquire the correct estimation of the RCS of aircrafts; however, no work has yet been proposed to establish relationship between RCS and reflection coefficient for ground-to-aircraft and satellite-to-aircraft communication scenarios. Moreover, no concrete relationship has been established so far between the RCS and SRC for a targeted body.

In this article, a new term named as Spatial Reflection Coefficient (SRC) is defined and then a concrete relationship of the interdependence between RCS and SRC is formulated. The relationship between RCS and SRC relates two different terms which are being used differently in two different fields of research. Both the terms are inter-dependent on each other and utilize the same input parameters like incidence angle, material properties, signaling frequency, polarization and observation angle. The RCS basically describes an effective area of a targeting object that intercepts the incoming signals transmitted through RADAR antenna and isotropically radiates the incident power in all directions. The ability of target's reflecting and its size are described with term RCS. However, on the other hand, the reflection coefficient is a qualitative parameter that describes surface reflecting ability and gives the amount of reflected electromagnetic wave due to impedance discontinuity in the transmission medium between the transmitter and receiver. The proposed relationship interrelates the RCS and the SRC which interchangeably help to extract the reflectivity information of a target's surface on the basis of observed RCS. Moreover, this interchangeability between the RCS and SRC will help researchers of the different fields and will allow them to utilize simulation tools and algorithms of both the domains interchangeably. For example, the researcher from the communication systems will be able to get the reflection properties of the scattering objects with the help of RADAR simulation tools. Aircraft's body reflecting/scattering properties are analyzed by designing geometrical models of two scenarios, satellite-to-aircraft and ground-to-aircraft. The proposed geometrical models help to evaluate the correct incident angles of incoming EM waves impinging on aircraft's surface. Bistatic RCS results are obtained by

incorporating a facet-based model of aircraft A380 and a simulation tool POFACET® [1]. For proposed geometrical models, bistatic RCS results are obtained and analyzed with respect to observation angles. Furthermore, the spatial reflection coefficients behavior is analyzed as a function of bistatic RCS and propagation distances of incoming and reflecting signals.

The rest of the paper is organized as follows. Section 2 presents methodology to develop a relationship between the RCS and SRC. The proposed geometry for two scenarios satellite-to-aircraft and ground-to-aircraft is presented in Section 3, to evaluate correct incident angles of impinging EM waves on the aircraft's body. In Section 4, the details of simulation tool and aircraft's facet-based model are given. In Section 5, simulation results of each incident angles evaluated in Section 3 are presented and analyzed in detail. Moreover, the behavior of the relationship between the RCS and SRC is also analyzed in Section 5. Finally, Section 6 concludes the paper.

II. RELATIONSHIP OF SPATIAL REFLECTION COEFFICIENT AND RCS

A. Radar cross section

In radar systems, RCS is a measure which defines the amount of scattered or reflected energy from the surface of a target towards the receiver antenna. If the locations of both the transmitter and receiver are identical then it is referred as monostatic RCS; however, in the cases when the locations are non-identical it is interpreted as Bistatic RCS (BRCS). Both the terms are identical in scattering methodology except the inclusion of bistatic angle in BRCS which makes it more complex than monostatic RCS. In terms of complex electric field amplitudes, the RCS (σ_B) is defined as follows [22,23]:

$$\sigma_B(\phi_i, \theta_i, \phi, \theta) = \lim_{R \rightarrow \infty} 4\pi R^2 \frac{|E_s|^2}{|E_i|^2}, \quad (1)$$

where, R is the distance between the target and the receiver antenna, and E_s and E_i are the complex amplitudes of the incident and the scattered electric fields respectively. Spherical angle coordinates (ϕ_i, θ_i) and (ϕ, θ) represents incident angles of incoming wave and reflected wave respectively.

B. Spatial reflection coefficient

In electromagnetic wave theory, reflection of a signal is one important phenomenon which occurs when the wave impinges on a reflective surface having a large dimension compared to its wavelength. When a signal reaches the receiver through different propagation paths, such environment is known as multipath environment. The relation between reflected and incident field is usually described by Fresnel equations, which depends upon the permittivity, conductivity of the surface and frequency, incident angle, polarization of the incident

wave. Reflection of a radio wave possesses directional property which can be further categorized into two types of reflections, specular reflection and diffuse reflection. In specular reflections, the angle of the reflected path is relatively constant to the angle of the incident wave; however, the diffuse reflections have random phase relative to the angle of the incident wave due to irregularities of the surface. In both the cases, the induced path loss varies on the basis of reflection coefficients which depends upon the dielectric characteristics of the reflective surface. For specular reflections, the path loss is obtained by using Fresnel equations while for diffused/scattered reflections a diffused scattering coefficient is multiplied with specular reflection coefficient [24-26]. The scattered reflections possess a unique spatial properties based upon reflecting angles of the wave from the scattering surface. Based upon the spatial characteristics of the scattered waves, we introduce a new parameter SRC as an addition to earlier terms elaborating reflection phenomenon of radio waves. SRC is defined as the ratio of the complex electric field intensity of the incident wave to that of the reflected wave electric field intensity in a specific direction:

$$\Gamma = \frac{E_s}{E_i}. \quad (2)$$

This can also be represented as:

$$\Gamma = \rho_0 e^{-j\theta}, \quad (3)$$

where, $\rho_0 = |\Gamma|$ represents magnitude of the spatial reflection coefficient and varies between $0 \leq \rho \leq 1$, θ is the phase angle of the reflection which presents phase change of the reflection and varies between $-\pi \leq \theta \leq \pi$. The amplitude value of the reflection coefficient is considered as a composite representation of three independent factors i.e reflection coefficient of smooth surface, roughness coefficient and diffusion factor. These three terms highly influence on the scattering properties of a surface and compositely defines the nature of a reflection coefficient [27].

C. Relationship of spatial reflection coefficient and RCS

Since Radar Cross Section and the spatial reflection coefficient are interdependent on each other; therefore, a relationship can be easily made between these two terms. Both RCS and SRC depend on the incidence angle, material properties, signaling frequency, polarization and observation angle. In order to develop a relation between RCS and SRC, we have assumed a typical bistatic geometry of signal reflection from the surface of an aircraft towards another aircraft present in the surroundings. As illustrated in Fig. 1, the aircraft (A_1) located at radial distance d_1 from radar transmitting antenna reflects the intercepted signal towards an aircraft (A_2) present at distance d_2 . Referring Fig. 1, the received power density at distance d_1 is calculated as:

$$P_d = \frac{P_t G_t}{4\pi d_1^2}, \quad (4)$$

where P_t denotes peak transmitted power and G_t is the gain of the radar transmitting antenna. Considering the methodology of bistatic radar cross section, the total reflected/scattered power received at aircraft (A_2) can be calculated as [28]:

$$(P_r)_{ref} = \frac{P_t G_t A_e \sigma_B(\phi_i, \theta_i, \phi, \theta)}{(4\pi)^2 d_1^2 d_2^2}, \quad (5)$$

where A_e is the effective aperture of the receiver antenna, σ_B is the bistatic RCS of the aircraft A_1 and d_2 is the distance/range of aircraft A_2 from A_1 . In terms of spatial reflection coefficient denoted by Γ , the total reflected/scattered power received at aircraft A_2 can be written as [24,25]:

$$(P_r)_{ref} = \frac{P_t G_t A_e \Gamma^2}{4\pi(d_1 + d_2)^2}. \quad (6)$$

Both the expressions presented in Eq. (5) and Eq. (6) are equivalent in nature and thus can be compared to formulate a relation between the RCS and SRC. Solving both expressions yields a final look of the relationship between the magnitude of spatial reflection coefficient (SRC) and RCS:

$$|\Gamma| = \frac{(d_1 + d_2)}{d_1 d_2} \sqrt{\frac{\sigma_B(\phi_i, \theta_i, \phi, \theta)}{4\pi}}. \quad (7)$$

From the expression, it is notable that SRC is directly proportional to the square root of the RCS multiplied by a constant multiple based upon the path lengths of incident and reflected path.

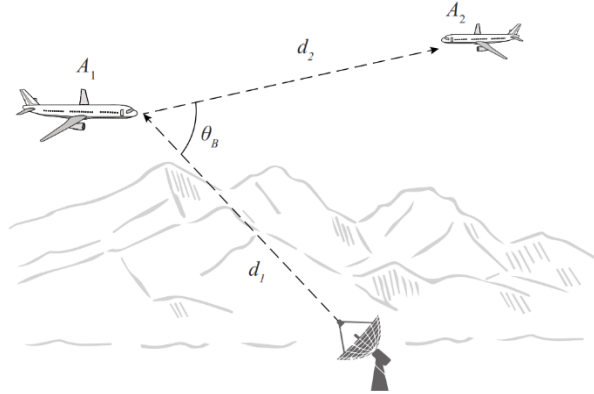


Fig. 1. An illustrative geometry of bistatic signal reflection from the surface of aircraft A_1 on to aircraft A_2 .

III. SYSTEM MODEL

A. Satellite-to-aircraft scenario

Communication through satellites is one effective resource of relaying radio signals between two different points on the earth, whether on the ground, at oceans or in the air. In recent years, satellites have become a

B. Ground-to-aircraft scenario

In order to observe scattering properties of a signal transmitted towards aircraft through ground wireless terminal/radar, a ground-to-aircraft scenario is assumed and presented in the Fig. 3. The Fig. 3 (a) explains the limitation of a LoS communication link due to spherical geometry of the Earth's surface. For clarity, a zoomed-in look of signal incidence and their corresponding angles with aircraft surface is illustrated in Fig. 3 (b). In this scenario, a wireless transmitter with three aircraft having the same altitude (h_A) present at three different positions are considered. The coverage range of a transmitter is denoted with a dotted circular ring in which an aircraft is considered to be detectable or could receive communication signals from ground transmitter. The aircrafts at position A and B are located at extreme/edge of the coverage range of the radar or the ground transmitter while the aircraft at position C is assumed to be located at the middle of the coverage range which is exactly above the transmitter. The maximum spread of the beamwidth can be obtained by knowing the altitude of the aircraft and the maximum radius $r_{C,max}$ of the coverage region. The angular spread of the beamwidth can be evaluated as follows [29]:

$$\Psi_B = 2 \tan^{-1} \left(\frac{r_{C,max}}{h_A} \right). \quad (14)$$

Where

$$r_{C,max} = \cos^{-1} \left(\frac{r_E}{r_E + h_A} \right). \quad (15)$$

The maximum angular span Ψ_B of beamwidth can then be evaluated as 176.8951° , by substituting $r_E = 6378.137^\circ$ km and $h_A = 10$ km in Eqs.(15) and (14). By utilizing the geometry presented in Fig. 3 (a), the incident angles α_A and α_B of EM waves impinging on aircraft A and B respectively are obtained as 1.5525° and 178.45° . Since, the aircraft A is located on the edge of the maximum coverage region; therefore, the angle α_A formed with the aircraft's surface is the minimum threshold angle below which the ground transmitter could not maintain a line of sight with the aircraft.

IV DESCRIPTION OF SIMULATION TOOL AND FACET-BASED MODEL OF AIRCRAFT A380

Physical Optics (PO) is one commonly used RCS prediction approach which provides best possible RCS results in the specular direction for electrically large complex bodies. It is a high-frequency simulation approach which is applicable in the situations when the wavelength of the incident wave is much smaller than the dimension of targeted body. In order to analyze scattering properties of incident EM waves on the surface of aircrafts, MATLAB-based Physical optics simulation tool

POFACET® 4.2 is used. In this tool, the RCS of a complex object is usually approximated by utilizing a large number of triangular meshes (facets) that collectively represents the continuous surface of the complex object. The total RCS of the object is then evaluated by the superposition of the square root of the magnitude of each individual facet's RCS. For our modeling, we choose A380 [27] the world's largest commercial aircraft as an example. For the designing of aircraft A380, AutoCAD® model (.dwg file) of aircraft A380 is obtained [30,31] within an accuracy of 10cm. The AutoCAD® software provides an opportunity to create a blueprint of any design to view it realistically before the continuation of the design process. A detailed description of aircraft A380 dimensions are shown in Fig. 4. Since, the POFACET® [1] simulation tool requires a facet-based model to predict RCS, therefore, AnyCAD software is used to generate facet-based model of aircraft A380. The facet-based representations of aircraft A380 are demonstrated in Fig. 5. Fig. 5 (a) and Fig. 5 (b) show top and bottom look of facet-based aircraft A380, which is the main requirement of our proposed model, while Fig. 5 (c) presents a side view of the aircraft. The steps of the gradational procedure involved in the calculation of the scattering properties of the aircraft are listed in Table 1.

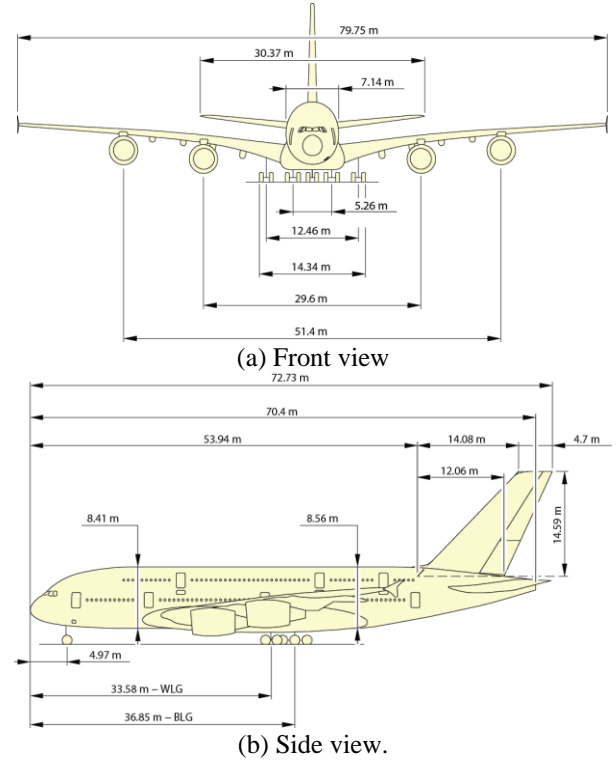


Fig. 4. Aircraft A380 detailed dimensions [27].

Table 1: Gradational procedure for the calculation of bistatic RCS

Gradational Algorithmic Procedure:	
1. Create an arbitrary aircraft model (aircraft.stl file format)	
2. Run pofacet.m	\\ GUI of POFACET® [1] will be shown
3. Select “Calculate Bistatic RCS”	\\ Options: Design Model Manually, \\ Design Model Graphically, \\ Calculate Monostatic RCS, \\ Calculate Bistatic RCS, Utilities
4. Select “Angle” for the calculation of bistatic RCS	\\ Options: Angle & Frequency
5. Load file (airplane.stl)	\\ Set view point if needed
6. Adjust incident angles range	\\ (θ_i, ϕ_i)
7. Set observation angles range	\\ $0^\circ \leq \theta_r^\circ \leq 360^\circ, 0^\circ \leq \phi_r^\circ \leq 360^\circ$
8. Adjust computational parameters	\\ Taylor series parameters, incident polarization \\ and frequency
9. Adjust surface roughness	\\ If required
10. Press the button “Calculate RCS”	
11. Select material type “ R_s ”	\\ Options: Surface resistivity values (R_s) or Material data
12. Get the output	

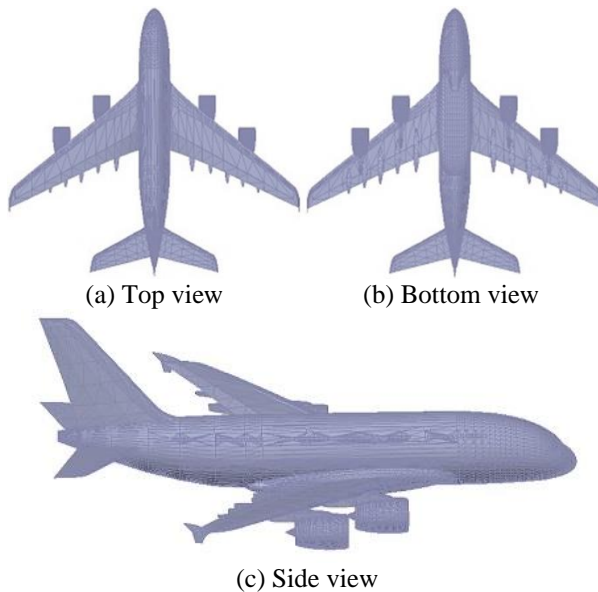


Fig. 5. Facet-based representation of aircraft A380.

V. SIMULATION RESULTS AND DISCUSSION

In this section, the RCS of aircraft A380 facet-based model is evaluated and analyzed for two scenarios: Satellite-to-aircraft and Ground-to-aircraft. For simulation process, three positions of aircrafts in both the scenarios are considered to compute bistatic RCS for specific incident angles as explained in Fig. 2 and Fig. 3 of Sec. III. The simulations of bistatic RCS are performed in spherical coordinate systems with incident angles (θ_i, ϕ_i) and observation angles (θ, ϕ) . The incident angle is considered to be fixed because in bistatic RCS cases the radar/transmitter is located at fixed angle to the targeting aircraft while the observation angle may vary. Therefore, it is not necessary to calculate bistatic RCS

for each incident angle. Although, the bistatic RCS can be observed in a wide range of observation angles equivalent to spherical geometry in the range $0 \leq \theta \leq \pi$ and $0 \leq \phi \leq 2\pi$; however, for simplicity only zero-azimuth plane (i.e., $\phi_i = 0, \phi = 0$) is considered to approximate bistatic RCS for the range of observation angle $0 \leq \theta \leq \pi$. The measured values can be represented easily in terms of bistatic angles by keeping the incident angles as a reference instead of an aircraft horizontal axis. In the scenario of Satellite-to-aircraft, only upper surface of the aircraft is considered for the evaluation of bistatic RCS, because a signal transmitted through satellite will encounter with only upper surface of the aircraft. The upper surface of the aircraft would be the main source of reflection and scattering of the signal towards the satellite or any other signal receiving entity. Similarly, in the scenario of ground-to-aircraft communication, the bottom surface of aircraft would be the main source of signal reflection/scattering at different observation angles towards the signal receiving units on the earth. In both the scenarios, the aircraft axis of motion (reflection plane) is considered as a reference for observation angles of bistatic RCS. The observation angles are measured in counter-clock wise rotation with reference to the reflection plane on the signal arrival side. For simulation, the number of Taylor series based polynomial is taken as 3, incident wave polarization mode is set at linear-vertical polarization, and the aircraft surface roughness is assumed as a smooth surface.

In satellite-to-aircraft communication link scenario, when both satellite and aircraft are present at the equator, the signal transmitted through satellite will make a 90 degrees angle with the aircraft upper body. In this case, the bistatic RCS fluctuations are obtained and plotted in Fig. 6 with respect to observation angle (θ) . The results are measured in counter-clock direction by keeping the horizontal axis of aircraft motion as a reference axis.

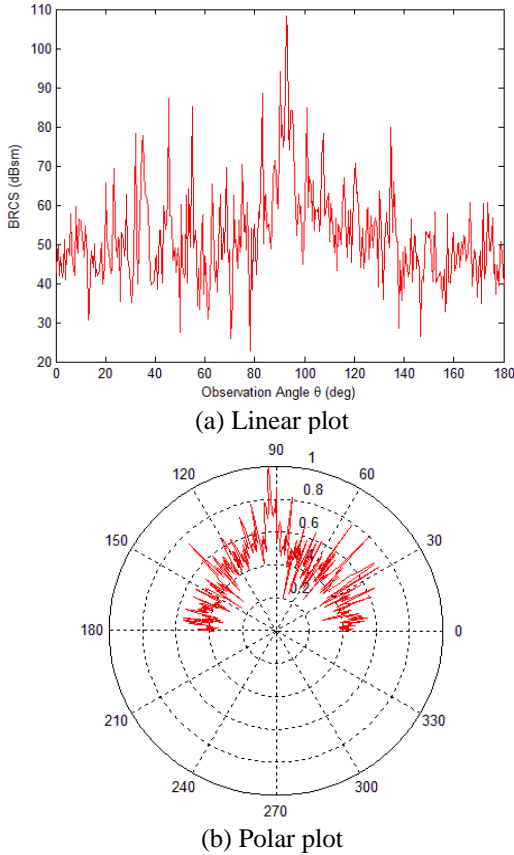


Fig. 6. RCS observation of signal incidence at $\beta_c = 90^\circ$ in satellite-to-aircraft communication scenario.

The RCS values are observed only at upper half region ($0 \leq \theta \leq 180$) of the observation angles because in this region the reflections would be prominent with high power gain. In the figure, a high peak is envisioned at angle 92.5° which is basically a specular reflection from the aircraft surface. Hence, at observation angles on which the BRCS is high, the reflecting surface of the aircraft will possibly provide strong interference to satellites or aircrafts located at these observation angles.

In Fig. 7, the angular bistatic scattering response of aircraft at incident angle $\beta_a = 21.921^\circ$ is shown with both linear and normalized polar plots in Fig. 7 (a) and Fig. 7 (b) respectively. The impact of signal incidence at angle β_a shows that the aircraft upper body scatters signal power in all directions with different power amplitudes. The specular reflection of aircraft is obtained at angle 158.079° with a power gain of 104.7 dBsm. Figure 8 presents scattering behavior of the aircraft surface for an incident angle of 158.079° with both linear and normalized polar graphs in Fig. 8 (a) and Fig. 8 (b) respectively.

The results show that at this particular incident angle the aircraft metallic surface and its curved structure scatters signal power in all directions with different

amplitude levels according to the observed angles θ . Specular reflection of the signal is observed at an angle of 22° with a power gain of 98.29 dBsm. From the simulation results, it can be concluded that in Satellite-to-aircraft communication links the aircraft metallic surface and its curved shape may provide interference to its surrounding receivers (satellite/aircrafts) due to signal reflections from its surface. In this situation, the performance of the surrounding receivers may get degraded based upon the interfering signal power level received at the receiver end. Hence, these simulation results provide a way to observe interfering signal reflections from flying aircrafts during the communication between satellites and aircrafts.

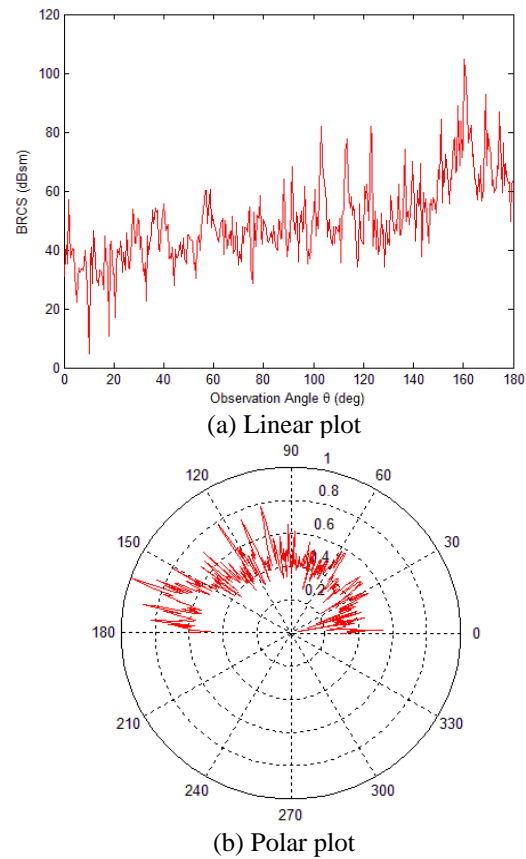


Fig. 7. RCS observation of signal incidence at $\beta_a = 21.921^\circ$ in satellite-to-aircraft communication scenario.

In Fig. 9, bistatic RCS of an aircraft by impinging a signal at incident angle $\alpha_c = 90^\circ$ to its lower body is evaluated and shown in both linear and polar plots. In the scenario of ground-to-aircraft, angular bistatic RCS observation are calculated by considering only the lower surface of aircraft. This is due to the fact that in this case the lower body of the aircraft would be the main source of signal reflection with high amplitude of scattering power as compared to the aircraft's upper surface.

Moreover, it is quite realistic to assume that in this scenario, the transmitted signals will not strike on the upper surface of the aircraft. By keeping the aircraft's axis of motion as a reference, angular bistatic RCS values are evaluated with respect to observation angles of range 0° to 180° in $\phi = 0$ plane, which is the lower half region of the aircraft in which the signal will scatter and carry the high scattering power. The observation angles are measured in the counter clock direction by keeping the aircraft's axis of motion as a reference axis, as shown in Fig. 9 (b). From the figure, it is worth notable that the lower part of the complex structure of aircraft constitutes good reflecting properties and generates signal reflection at every observation angle which are considered in this simulation. In the figure, the highest peak of bistatic RCS is observed at 131.5° with 90.29 dBsm amplitude, however, the specularly reflected RCS amplitude value is obtained as 87.72 dBsm at angle 87.5° . The high peaks other than the specularly reflected power occur due to the complex curved structure of the aircraft's metallic body which reflects/scatters incident wave towards these particular observation angles and as a result gives rise to bistatic RCS.

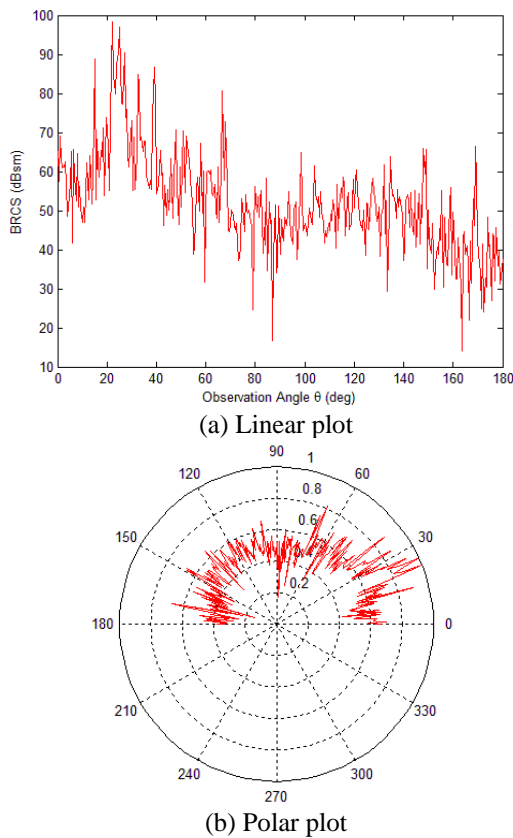


Fig. 8. RCS observation of signal incidence at $\beta_B = 158.079^\circ$ in satellite-to-aircraft communication scenario.

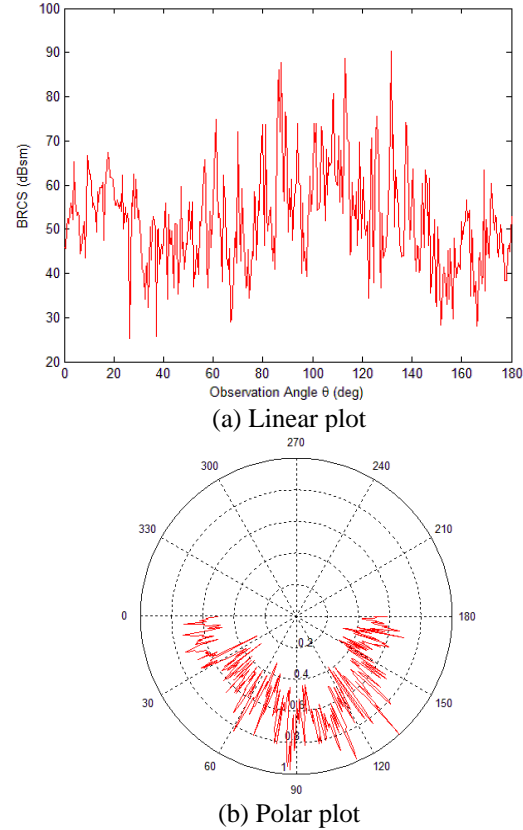


Fig. 9. RCS observation of signal incidence at $\alpha_C = 90^\circ$ in ground-to-aircraft communication scenario.

In Fig. 10, bistatic RCS of aircraft at incident angle $\alpha_A = 1.5525^\circ$ is presented with both linear and polar graphs in Fig. 10 (a) and Fig. 10 (b) respectively. The bistatic RCS shows specularly reflected behavior at an angle 179.5° with amplitude 87.21 dBsm. In Fig. 11, bistatic RCS of the impinging wave having incident angle $\alpha_B = 178.45^\circ$ with respect to observation angles θ is presented. The maximum value of bistatic RCS is observed at angle 2° with amplitude 81.59 dBsm. Bistatic RCS observations of these incident angles give a way to envision the interfering reflected power from the aircraft's surface which degrades the performance of neighboring receivers whether aircrafts or ground terminals. By keeping the knowledge of interfering signal power, counter-measures can be made for better performance and error avoidance.

Figure 12 presents the behavior of spatial reflection coefficient as a function of RCS, line-of-sight (LOS) distance (d_1) and reflected signal distance (d_2). For simulation, bistatic RCS results obtained in satellite-to-aircraft scenario with 90° signal incidence are only used. Whereas, the LOS distance (d_1) and reflected signal distance (d_2) are taken as 35786 km and 10 km

respectively. The result explains that how much power is reflected from the surface of the aircraft and as a result providing interfering signal reflection to its neighboring receivers. At 90° signal incidence from the satellite, the aircraft surface will provide a strong reflection to aircrafts/satellites which are present at 90° observation angle, however, it will provide quite ignorable interference at rest of the observation angle. Varying the distances of LOS (d_1) and reflected signal paths (d_2), the behavior of spatial reflection coefficient can be envisioned in Fig. 13.

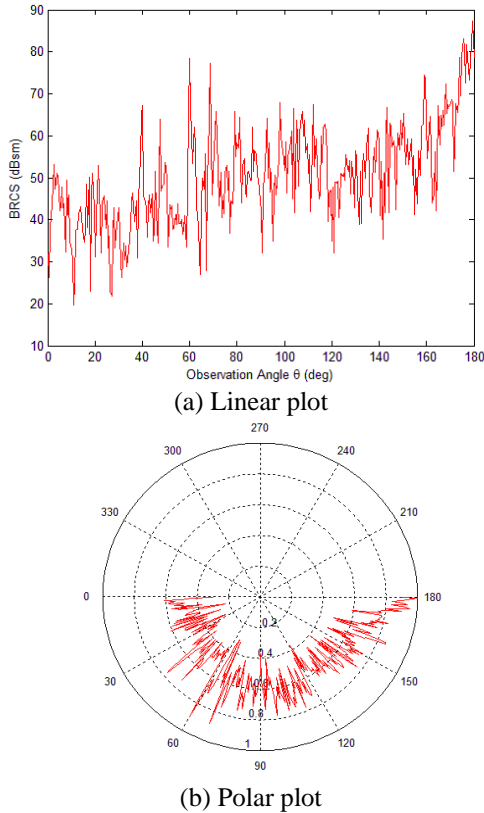


Fig. 10. RCS observation of signal incidence at $\alpha_A = 1.5525^\circ$ in ground-to-aircraft communication scenario.

From the figure, it is observable that the amplitude of SRC decreases as the distance increases and increases when the distances decrease. The results show a way to observe the scattering mechanism of a signal from flying aircrafts and strength of reflected interfering signal. A comparison between SRC and RCS is shown in the Fig. 14. Comparison between SRC and RCS shows that both the terms follows the same trend with a constant scaling factor based upon the propagation distances. From the analysis, it is observed that SRC and RCS follow the same scattering behavior and can be used interchangeably to analyze a communication system model. In wireless communication systems, multipath environment is a propagation phenomenon which occurs due to reflection,

diffraction, refraction or scattering of a signal through objects (scatters) present between the transmitter and receiver. In such environments, the receiver receives multiple versions of phase shifted and attenuated signals, which when combined results a faded signal of much less power. Thus, the RCS can be used interchangeably instead of reflection coefficient to validate and analyze any communication system model. From the design and simulation point of view, as POFACET [1] simulation tool works by utilizing a facet-based representation of a model, therefore, inaccurate facet-based modeling of a model may induce facetization error which may lead to inaccurate observation of the RCS. The facetization error usually occurs when a smooth continuous surface is represented by discrete facets having inappropriate size (i.e., large facets) as compared to the smoothness of the surface. Hence, to decrease the facetization error, an appropriate mesh size must be used to generate a tight fitting mesh representation of the model. On one hand, accurate calculations of bistatic RCS require a smooth facet-based model with small facet size, while on the other hand, this leads to high computations which is not always possible to perform on normal computers. Therefore, a machine having a high-processing capability may get more accurate RCS results with less facetization error.

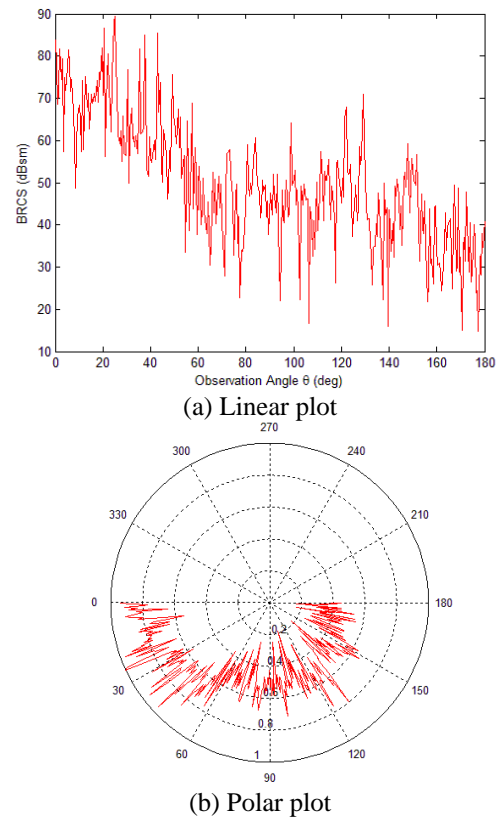


Fig. 11. RCS observation of signal incidence at $\alpha_B = 178.45^\circ$ in ground-to-aircraft communication scenario.

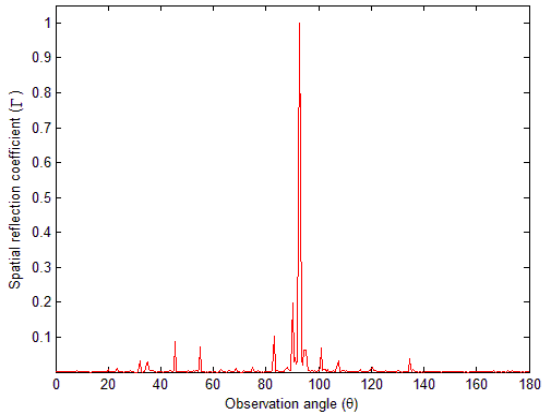


Fig. 12. Plot of spatial reflection coefficient as a function of bistatic RCS formulated with 90° signal incidence in satellite-to-aircraft scenario.

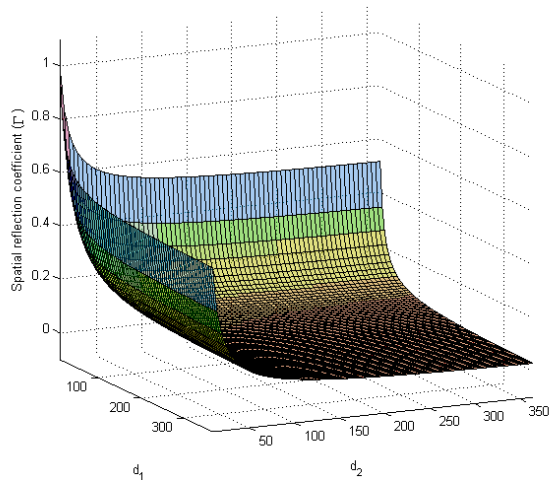


Fig. 13. Reflection coefficient as a function of RCS, d_1 and d_2 .

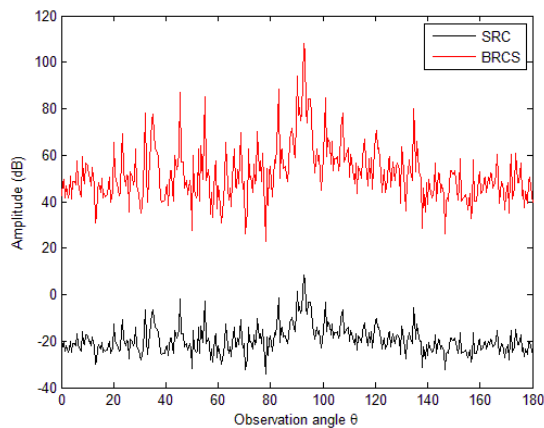


Fig. 14. Comparison between SRC and BRCS.

VI. CONCLUSION

Correct evaluation of the RADAR Cross Section (RCS) and its prediction is imperative in designing of high performance radars as well as for aircrafts having low visibility towards the radar. In this article, interdependence of the RCS and Spatial Reflection Coefficient (SRC) has been highlighted to formulate a compact relationship between the two terms. Scattering mechanism of aircraft surface has been analyzed by developing geometrical models of two scenarios, i.e., satellite-to-aircraft and ground-to-aircraft. The proposed geometrical models were developed to obtain incident angles of impinging EM waves on the surface of the aircraft. In order to observe the bistatic RCS of aircraft, POFACET® [1] simulation tool has been incorporated with a facet-based model of aircraft A380. From the simulations, it was observed that complex structure of aircraft model constitutes good reflecting properties which in turn may provide interfering signals to its neighboring aircrafts which may degrades their communication performance. From the results, it was concluded that accurate geometrical modeling of aircraft communication environment may help to understand the nature of interfering signals and to increase the communication performance in satellite-to-aircraft and ground-to-aircraft communication systems. Analysis shows that SRC and RCS can be used interchangeably which may help to analyze and validate the communication system models for better performance. The conceptual relationship between SRC and RCS is analyzed on the basis of the data taken from simulations. Since no measurements are incorporated; hence, the conclusive observations are just indicative but not definitive. In future, a more generalized aircraft scattering geometrical model should be established to observe the scattering behavior of signals from aircraft surface in 3D space.

REFERENCES

- [1] F. Chatzigeorgiadis and D. C. Jenn, "A matlab physical-optics rcs prediction code," *IEEE Antennas and Propagation Magazine*, vol. 46, no. 4, pp. 137-139, 2004.
- [2] X. Fan, Y. Qin, S. Shang, D. Song, W. Sun, D. Li, and X. Luo, "Research on the bastatic rcs characteristics of stealth aircraft," *Asia-Pacific Microwave Conference (APMC)*, vol. 3, pp. 1-3, Dec. 2015.
- [3] L. Zhu, X. Liang, J. Li, and R. Li, "Simulation analysis on static scattering characteristics of stealth aircraft," *IEEE Advanced Information Management, Communicates, Electronic and Automatic Control Conference (IMCEC)*, pp. 1774-1778, Oct. 2016.
- [4] J. M. Jin, *Theory and Computation of Electromagnetic Fields*. John Wiley & Sons, 2011.

- [5] E. Mach, *The Principles of Physical Optics: An Historical and Philosophical Treatment*. Dover, NY, USA, 1953.
- [6] D. Jenn and C. Ton, "Wind turbine radar cross section," *International Journal of Antennas and Propagation*, vol. 2012, p. 14, 2012.
- [7] A. Ishimaru, *Electromagnetic Wave Propagation, Radiation and Scattering*. Englewood Cliffs, New Jersey, Prentice Hall, 1991.
- [8] J. Song, C.-C. Lu, and W.C. Chew, "Multilevel fast multipole algorithm for electromagnetic scattering by large complex objects," *IEEE Transaction on Antennas and Propagation*, vol. 45, no. 10, pp. 1488-1493, Oct. 1997.
- [9] G. Cakir, M. Cakir and L. Sevgi, "Radar cross section (rcs) modeling and simulation, part 2: A novel fdtd-based rcs prediction virtual tool for the resonance regime," *IEEE Antennas and Propagation Magazine*, vol. 50, no. 2, pp. 81-94, Apr. 2008.
- [10] G. Cakir, M. Cakir, and L. Sevgi, "An FDTD-based parallel virtual too for rcs calculations of complex targets," *IEEE Antennas and Propagation Magazine*, vol. 56, no. 5, pp. 74-90, Oct. 2014.
- [11] L. Sevgi, "Target reflectivity and rcs interactions in integrated maritime surveillance systems based on surface-wave high-frequency radars," *IEEE Antennas and Propagation Magazine*, vol. 43, no. 1, pp. 36-51, Feb. 2001.
- [12] J. D. Wilson, "Probability of detecting aircraft targets," *IEEE Transactions on Aerospace and Electronic Systems*, no. 6, pp. 757-761, 1972.
- [13] A. David, C. Brousseau, and A. Bourdillon, "Simulations and measurements of a radar cross section of a Boeing 747-200 in the 20-60 mhz frequency band," *Radio Science*, vol. 38, no. 4, pp. 3-1-3-4, 2003.
- [14] B. Persson and M. Norsell, "On modeling rcs of aircraft for flight simulation," *IEEE Antennas and Propagation Magazine*, vol. 56, no. 4, pp. 34-43, 2014.
- [15] Z. W. Liu, D. Z. Ding, Z. F. Fan, and R. S. Chen, "Adaptive sampling bicubic spline interpolation method for fast calculation of monostatic rcs," *Microwave and Optical Technology Letters*, vol. 50, no. 7, pp. 1851-1857, 2008. [Online]. Available: <http://dx.doi.org/10.1002/mop.23540>
- [16] Z. W. Liu, R. S. Chen, and J. Q. Chen, "Adaptive sampling cubic-spline interpolation method for efficient calculation of monostatic rcs," *Microwave and Optical Technology Letters*, vol. 50, no. 3, pp. 751-755, 2008.
- [17] W.-D. Li, J.-X. Miao, J. Hu, Z. Song, and H.-X. Zhou, "An improved cubic polynomial method for interpolating/extrapolating mom matrices over a frequency band," *Progress in Electromagnetics Research*, vol. 117, pp. 267-281, 2011.
- [18] W.-D. Li, H.-X. Zhou, J. Hu, Z. Song, and W. Hong, "Accuracy improvement of cubic polynomial inter/extrapolation of mom matrices by optimizing frequency samples," *IEEE Antennas and Wireless Propagation Letters*, vol. 10, pp. 888-891, 2011.
- [19] Y. An, D. Wang, and R. Chen, "Improved multilevel physical optics algorithm for fast computation of monostatic radar cross section," *IET Microwaves, Antennas & Propagation*, vol. 8, no. 2, pp. 93-98, 2014.
- [20] T. S. Rappaport, *Wireless Communications: Principles and Practice*. Prentice Hall PTR New Jersey, vol. 2, 1996.
- [21] R. Geise, A. Enders, H. Vahle, and H. Spieker, "Scaled measurements of instrument-landing-system disturbances due to large taxiing aircraft," *IEEE Transactions on Electromagnetic Compatibility*, vol. 50, no. 3, pp. 485-490, 2008.
- [22] E. F. Knott, *Radar Cross Section Measurements*. Springer US, 1993.
- [23] M. Cherniakov, *Bistatic Radar: Principles and Practice*. John Wiley & Sons Ltd, 2007.
- [24] O. Landron, M. J. Feuerstein, and T. S. Rappaport, "In situ microwave reflection coefficient measurements for smooth and rough exterior wall surfaces," *43rd IEEE Vehicular Technology Conference*, pp. 77-80, 1993.
- [25] O. Landron, M. J. Feuerstein, and T.S. Rappaport, "A comparison of theoretical and empirical reflection coefficients for typical exterior wall surfaces in a mobile radio environment," *IEEE Transactions on Antennas and Propagation*, vol. 44, no. 3, pp. 341-351, 1996.
- [26] S. R. Bullock, *Transceiver and System Design for Digital Communications*. SciTech Publishing Inc., 2009.
- [27] J. Liu, *Spacecraft TT&C and Information Transmission Theory and Technologies*. Springer-Verlag Berlin Heidelberg, 2015.
- [28] B. Mahafza, *Introduction to Radar Analysis*, ser. Advances in Applied Mathematics Series. Taylor & Francis, 1998. [Online]. Available: <https://books.google.com.pk/books?id=HnbERpIIX0C>
- [29] S. J. Nawaz, N. M. Khan, M. I. Tiwana, N. Hassan, and S. I. Shah, "Airborne internet access through submarine optical fiber cables," *IEEE Transactions on Aerospace and Electronic Systems*, vol. 51, no. 1, pp. 167-177, 2015.
- [30] Airbus S.A.S, "Aircraft characteristics airport and maintenance planning," 01 Dec 2016. [Online]. Available: <http://www.airbus.com/support-services/support/technical-data/aircraft-characteristics/>
- [31] Airbus S.A.S, "Autocad 3-view aircraft drawings," 10 May 2012. [Online]. Available: <http://www.airbus.com/support-services/support/technical->

data/autocad-3view-aircraft-drawings/



Muhammad-Yasir Masood Mirza received his M.Sc. Mathematics degree from International Islamic University, Islamabad, Pakistan in 2006 and the M.S. Electronics Engineering degree with specialization in Communication Systems from Mohammad Ali Jinnah

University, Islamabad, Pakistan in 2011. At present, he is pursuing his Doctoral Degree from Capital University of Science and Technology (CUST), Islamabad, Pakistan. His research interests include channel modeling and characterization, channel estimation, smart antenna systems, localization and ground-to-air communication systems.



Noor M. Khan received his B.Sc. degree in Electrical Engineering from the University of Engineering and Technology (UET), Lahore, Pakistan, in 1998 and Ph.D. degree in Electrical Engineering from the University of New South Wales (UNSW), Sydney, Australia in 2006.

He held several positions in WorldCall, NISTE, PTCL, UNSW, GIK Institute of Engineering Sciences and Technology, and Mohammad Ali Jinnah University, Pakistan from 1998 to 2015. Currently, he is working as Professor with the Capital University of Science & Technology (CUST), Islamabad, Pakistan. He has served as Chair and Co-Chair of the Technical Program Committees of IEEE International Conference on Emerging Technologies (ICET2012) in 2012 and IEEE International Multi-topic Conference (INMIC-2009) in 2009, respectively. He has been awarded Research Productivity Award (RPA) by the Pakistan Council for Science and Technology (PCST) for the years 2011 and

2012. His research interests include channel modeling and characterization, wireless sensor networks, cellular mobile communication networks and ground-to-air communication systems.



Abid Jamal was born in Pakistan in 1991. He received the B.Sc. degree in Electronic Engineering from the University of Lahore, Islamabad, Pakistan and M.S. in Electrical Engineering from Capital University of Science and Technology, Islamabad, Pakistan in 2016. His research

interests include Radar cross section measurements, smart grid communication, cellular and mobile communication systems.



Rodica Ramer received a B.Sc. degree in Engineering Physics, M.E. in Electrical Engineering and Ph.D. in the Solid State Physics in 1989, all from the University of Bucharest. Ramer joined the University of New South Wales (UNSW), in 1993, where she is a Professor in the

School of Electrical Engineering and Telecommunications, leading the micro-wave, millimeter-wave and electromagnetics group. She has held guest and visiting professorship positions at many Universities around the world. Her research activities have been in the area of microwave devices and materials and EM techniques. She has authored and co-authored over 250 refereed papers and a number of book/chapters and patents. Her current research involves advancements in RF MEMS and SIW technologies. Ramer is a Senior Member of IEEE MTT-S, AP-S and Com.Soc., and a Fellow of Electromagnetics Academy. She has held key positions and has served on various panels and international committees and international conferences/symposia. She has served on editorial/review boards of several journals and conferences.